

Novel precursors for boron nanotubes: the competition of two-center and three-center bonding

Hui Tang and Sohrab Ismail-Beigi

Department of Applied Physics, Yale University, New Haven, CT 06520

(Dated: October 24, 2018)

We present a new class of boron sheets, composed of triangular and hexagonal motifs, that are more stable than structures considered to date and thus are more likely to be the precursors of boron nanotubes. We describe a simple and clear picture of electronic bonding in boron sheets and highlight the importance of three-center bonding and its competition with two-center bonding, which can also explain the stability of recently discovered boron fullerenes. Our findings call for reconsideration of the literature on boron sheets, nanotubes and clusters.

PACS numbers: 61.46.-w, 68.65.-k, 73.22.-f, 73.63.Fg

All boron nanotubes (BNT), regardless of diameter or chirality, are predicted to be metallic and have large densities of states (DOS) at their Fermi energies (E_F) [1]. In contrast, carbon nanotubes (CNT) can be semiconductors or metals with small DOS at their E_F . Metallic CNT are used widely to study one-dimensional (1D) electronics [2, 3] and are superconducting at low temperatures [4, 5]. Due to the larger DOS, BNT should be better metallic systems for 1D electronics and may have higher superconducting temperatures than CNT.

Recent experiments have fabricated boron nanotubular structures both as small clusters [6] and long, 1D geometries [7]. Understanding the properties of BNT is crucial for realizing their applications. For CNT, it has been fruitful to study two-dimensional (2D) graphene: *e.g.*, many properties of CNT are derived directly from graphene [8, 9]. For boron, however, no 2D planar structure exists in its crystals which are built from B_{12} icosahedra [10]. Researchers have proposed several 2D boron sheets (BS). The hexagonal graphitic BS was found to be unstable [11, 18]. Based on extensive theoretical studies of boron clusters [11, 12, 13, 14, 15], an Aufbau principle was proposed whereby the most stable structures should be composed of buckled triangular motifs [12]. Experiments on small clusters of 10-15 atoms support this view [16]. A recent study of many possible sheet structures found, again, the buckled triangular arrangement to be most favorable [17]. Hence, 2D triangular BS have been studied and used to construct BNT [18, 19, 20].

In this Letter, we present a class of boron sheets that are more stable than the currently accepted ones. We describe their structures, energetics, electronic states, and provide a clear picture of the nature of their bonding that clarifies their stability. We also show that clusters with these structures are competitive with or more favorable than those considered to date. Our findings have important consequences for understanding and interpreting the properties of these systems. For example, the unusual stability of B_{80} fullerenes [21] can be explained by our bonding picture. Hence, in our view, it is necessary to reconsider previous work in this general field.

We use Density Functional Theory [22, 23] within the *ab initio* supercell planewave pseudopotential total en-

ergy approach [24]. Calculations are done by PARATEC [25]. We use both the local density approximation (LDA) [23, 26] and the generalized gradient approximation (GGA) [27] for exchange and correlation. Most results below employ the LDA and key results are checked by the GGA. The LDA and GGA yield same qualitative results with minor quantitative variances. The planewave basis has a 32 Ryd cutoff energy. K-point samplings for each case converge total energies to better than 1 meV/atom. Norm-conserving pseudopotentials have cutoff radii $r_c^s=1.7$ and $r_c^p=2.1$ a.u.. The BS are extended in x-y directions while supercells have periodic copies along z where a separation of 7.4 Å is sufficient for convergence. For all structures, relaxations are performed until the atomic Hellmann-Feynman forces are less than 1 meV/Å and all in-plane stresses are less than 5 MPa.

Table I shows our results for four different sheets: the flat and buckled triangular sheets [18, 19], the hexagonal sheet, and one of our sheets (α in Figure 1). The hexagonal sheet is unstable with respect to in-plane shear, so we obtain the values in Table I by maintaining hexagonal symmetry while optimizing the bond length. The

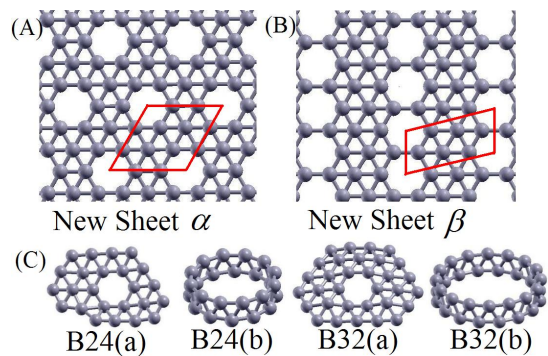


FIG. 1: (A, B) Two examples of our BS (top view). Red solid lines show the unit cells. (C) Four boron clusters: $B_{24}(a)$ and $B_{32}(a)$ are clusters with hexagonal holes; $B_{24}(b)$ and $B_{32}(b)$ are the double-ring clusters from refs. [14, 15]. Gray balls are boron atoms, and gray “bonds” are drawn between nearest neighbors.

TABLE I: Binding energies E_b (in eV/atom) and geometric parameters (in Å) of four BS: the flat and buckled triangular sheets, the hexagonal sheet, and one of our sheets (α in Figure 1). d^{flat} is the bond length of the flat triangular sheet. d^σ and d^{diag} are the bond lengths of the buckled triangular sheet, d^σ is between atoms with the same z , while d^{diag} is between atoms with different z . Δz is the buckling height. d^{hex} is the bond length for the hexagonal sheet. d^{new} gives the bond length range in the sheet α .

	Flat triangular		Buckled triangular			
	E_b	d^{flat}	E_b	d^σ	d^{diag}	Δz
LDA	6.58	1.68	6.74	1.59	1.80	0.81
previous LDA[19]	6.76 ^a	1.69	6.94 ^a	1.60	1.82	0.82
previous LDA[18]	6.53	-	6.79	-	-	-
GGA	5.79	1.70	6.00	1.60	1.86	0.88
previous GGA[17]	5.48 ^b	1.71	5.70 ^b	1.61	1.89	-
	Hexagonal		Sheet α			
	E_b	d^{hex}	E_b	d^{new}		
LDA	5.82	1.65	6.86	1.64-1.67		
GGA	5.25	1.67	6.11	1.66-1.69		
previous GGA[17]	4.96 ^b	1.68	-	-		

^aBoron’s atomic spin-polarization energy of 0.26 eV/atom explains the E_b differences between [19] and our work or [18].

^bWhile the absolute E_b from [17] do not match our GGA results, E_b differences among the sheets match very well.

binding energy is

$$E_b = E_{at} - E_{sheet},$$

where E_{at} is the energy of an isolated spin-polarized boron atom and E_{sheet} is the energy per atom of a sheet. The buckled triangular sheet is more stable than the flat one due to the former forming stronger σ bonds along the buckled direction [19]. We also can reproduce previous results on BNT made from triangular sheets [18, 19].

Figure 1 shows two examples of our BS, which are more stable than the buckled triangular sheet by 0.12 (α) and 0.08 (β) eV/atom. All our sheets are metallic, flat and composed of mixtures of hexagons and triangles. Sheet α is the most stable structure in our library.

Our sheets can be obtained by removing certain atoms from a flat triangular sheet. Each removal produces a hexagonal hole, generating a mixture of hexagons and triangles. We define a “hexagon hole density”

$$\eta = \frac{\text{No. of hexagon holes}}{\text{No. of atoms in the original triangular sheet}}.$$

The triangular sheet has $\eta=0$, the hexagonal $\eta=1/3$, and sheets α and β have η of $1/9$ and $1/7$, respectively.

A priori, the energies of these sheets can depend on both η and the pattern of hexagons. This results in a huge phase space of hexagonal patterns for a given η . The most stable structures occur when the hexagons are distributed as evenly as possible at fixed η . Figure 2 shows the LDA binding energies E_b versus η for this class of structures. E_b reaches a maximum of 6.86 eV/atom at $\eta=1/9$ (sheet α). We also have investigated the other

extreme where hexagons form lines (*e.g.*, sheet β). These “linear” structures are more stable than the buckled triangular sheet for $\eta \approx 1/9$ but are less stable than the “evenly-distributed” class described above.

To explain the stability of these structures, we describe the nature of their electronic bonding. Generally, in-plane bonds formed from overlapping sp^2 hybrids are stronger than out-of-plane π -bonds derived from p_z orbitals, so a structure that optimally fills in-plane bonding states should be most preferable. Guided by this principle, Figure 3 shows projected densities of states (PDOS) for five BS with separate in-plane (the sum of s , p_x and p_y) and out-of-plane (p_z) projections.

We begin with the hexagonal sheet, a textbook sp^2 bonded system. All sp^2 hybrids are oriented along nearest neighbor vectors so that overlapping hybrids produce canonical two-center bonds. A large splitting ensues between in-plane bonding and anti-bonding states. The p_z orbitals form their own manifold of bonding and anti-bonding states. The p_z PDOS vanishes at the transition point between the two. In the case of graphene, the four valence electrons per atom completely fill the sp^2 and the p_z bonding states, leading to a highly stable structure. However, a boron atom has only three valence electrons. As shown in Figure 3, some of the strong in-plane sp^2 bonding states are unoccupied, explaining the instability of this sheet. For our discussion below, this sheet is highly prone to accepting electrons to increase its stability should they be available from another source.

Next, we consider the flat triangular sheet. Each atom has six nearest neighbors but only three valence electrons. No two-center bonding scheme leads to a proper description. Previous work has noted qualitatively that a three-center bonding scheme exists here [19]. We now present a detailed model of the three-center bonding with crucial implications for the stability of our sheets. Figure 4 shows a choice of orientations for the sp^2 hybrids

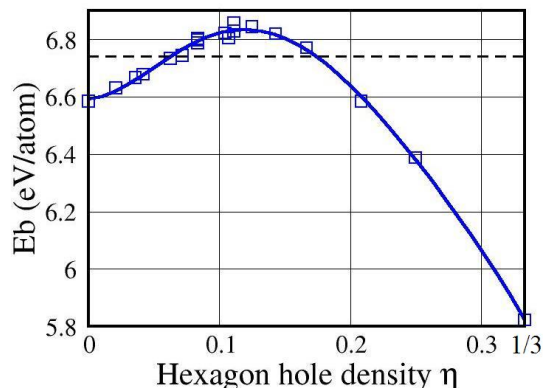


FIG. 2: LDA E_b v.s. hexagon hole density η for sheets with evenly distributed hexagons. The dashed line shows E_b for the buckled triangular sheet. The solid blue curve is a polynomial fit. The two limiting cases $\eta = 0$ and $\eta = 1/3$ correspond to the flat triangular and hexagonal sheets, respectively. Maximum E_b occurs for sheet α ($\eta = 1/9$).

where three hybrids overlap within an equilateral triangle formed by three neighboring atoms. For an isolated such triangle, we have a simple 3×3 tight-binding problem with D_3 symmetry. Its eigenstates are dictated by group theory: one low-energy symmetric bonding orbital b and two degenerate high-energy anti-bonding orbitals a^* . (This is “closed” three-center bonding; details on this and other types of bonds are found in standard references [28].) These orbitals then broaden into bands due to inter-triangle couplings. Separately, the p_z orbitals also broaden into a single band (not shown). In Figure 3, the in-plane PDOS becomes zero at the energy separating in-plane bonding and anti-bonding states. Ideally this sheet would be most stable if: (i) two electrons per atom would

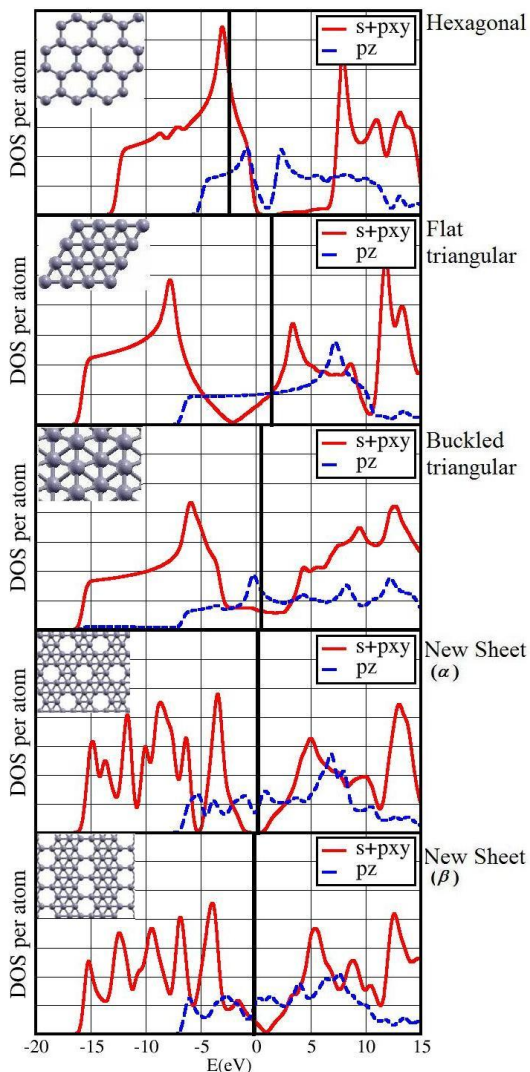


FIG. 3: Projected Densities of States (PDOS) for four BS. DOS are projected to in-plane (sum of s , p_x and p_y) and out-of-plane orbitals (p_z). Red solid lines show in-plane and blue dashed lines show out-of-plane projections; thick vertical solid lines show E_F . All curves are broadened using Gaussians with a width of 0.3 eV. The vertical scale is arbitrary.

completely fill the b -derived in-plane bonding bands, (ii) the anti-bonding a^* -derived bands were empty, and (iii) the remaining electron per atom would half fill the low-energy (bonding) portion of the p_z -derived band. This would mean that the E_F would be at the zero point of the in-plane PDOS in Figure 3. Clearly, this picture is a valid zeroth-order description. However, E_F lies slightly above the ideal position and makes some electrons occupy in-plane anti-bonding states. In other words, this sheet prefers to donate these high-energy electrons which has critical implications below. (Although we seem to break symmetry by making half of the triangles filled and half empty, filling the entire b -derived in-plane bonding band makes all hybrids equally occupied. This restores full in-plane symmetry: *i.e.*, the two possible initial orientations of hybrids give the same final state.)

The flat triangular sheet, however, buckles under small perturbations along z [18]. The buckling mixes in-plane and out-of-plane states and can be thought of as a symmetry reducing distortion that enhances binding. As shown in Figure 3, some states move below the E_F as indicated by the small peak immediately below the E_F .

Finally, we turn to the new structures. The above discussion has shown that the hexagonal sheet should be able to lower its energy by accepting electrons while the flat triangular structure has a surplus of electrons in anti-bonding states. From a doping perspective, the three-center flat triangular regions should act as donors while the two-center hexagonal regions act as acceptors. Thus if the system is able to turn into a mixture of these two phases in the right proportion, it should be able to benefit from the added stability of both subsystems. Specifically, the hexagon-triangle mixture with the highest stability should be the one that places the E_F precisely at the zero-point of in-plane PDOS, filling all available in-plane bonding states and none of the anti-bonding ones. The remaining electrons will fill the low-energy p_z -derived states, leading to a metallic system. These expectations are born out clearly in Figure 3 as well as in the energetic stability of the various structures (Figure 2). In fact, the most stable sheet, α , satisfies this condition precisely while the less stable sheet, β , has a slight shift of E_F from the ideal position.

These findings have ramifications for boron clusters. Our structures and bonding picture can explain that the extreme stability of B_{80} fullerenes composed of triangular motifs with pentagonal holes [21] is due to the well

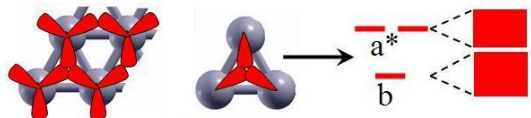


FIG. 4: Three-center bonding scheme in flat triangular sheets. Left: orientation of sp^2 hybrids. Center and right: overlapping hybrids within a triangle (D_3 symmetry) yield one bonding (b) and two anti-bonding (a^*) orbitals. These then broaden into bands due to inter-triangle interactions.

balance of three-center and two-center bonds. Also the α sheet can be seen as the precursor of B_{80} just as graphene is the precursor of carbon fullerenes. We also have studied some clusters. Figure 1 shows the double-ring structures for B_{24} and B_{32} [14, 15] along with clusters constructed by us. The new B_{24} cluster with a hexagon hole is less favorable by 0.08 eV/atom while the B_{32} is *more* favorable by 0.03 eV/atom than the corresponding double-ring. The stability of our sheets, of B_{80} , and our clusters with hexagonal holes suggests that for boron systems with more than 20-30 atoms, the Aufbau principle breaks

down and a more general structural rule is required.

In brief, we demonstrate a novel bonding mechanism in pure boron compounds arising from the competition between two- and three-center bonding. This explains the stability of our boron sheets as well as larger boron clusters. Our results have relevant implications on the stability and structure of boron clusters, boron nanotubes, and other boron systems.

We thank the Bulldog parallel clusters of the Yale High Performance Computing center for providing computational resources.

-
- [1] I. Boustani and A. Quandt, *Europh. Lett.* **39**, 527 (1997).
 [2] S. J. Tans, *et al.*, *Nature* **386**, 474 (1997).
 [3] M. Bockrath, *et al.*, *Science* **275**, 1922 (1997).
 [4] M. Kociak, *et al.*, *Phys. Rev. Lett.* **86**, 2416 (2001).
 [5] I. Takesue, *et al.*, *Phys. Rev. Lett.* **96**, 57001 (2006).
 [6] B. Kiran, *et al.*, *PNAS* **102**, 961 (2005).
 [7] D. Ciuparu, *et al.*, *J. Phys. Chem. B* **108**, 3967 (2004).
 [8] N. Hamada, S. Sawada, and A. Oshiyama, *Phys. Rev. Lett.* **68**, 1579 (1992).
 [9] R. A. Jishi, L. Venkataraman, M. S. Dresselhaus, and G. Dresselhaus, *Chem. Phys. Lett.* **209**, 77 (1993).
 [10] E. L. Muetterties, *The Chemistry of Boron and its Compounds* (Wiley & Sons, New York, 1967).
 [11] I. Boustani, A. Quandt, E. Hernandez, and A. Rubio, *J. Chem. Phys.* **110**, 3176 (1999).
 [12] I. Boustani, *Phys. Rev. B* **55**, 16426 (1997).
 [13] I. Boustani, *Surf. Sci.* **370**, 355 (1999).
 [14] S. Chacko, D. G. Kanhere, and I. Boustani, *Phys. Rev. B* **68**, 035414 (2003).
 [15] I. Boustani, A. Rubio, and J. A. Alonso, *Chem. Phys. Lett.* **311**, 21 (1999).
 [16] H. J. Zhai, B. Kiran, J. Li, and L. S. Wang, *Nat. Mater.* **2**, 827 (2003).
 [17] K. C. Lau, and R. Pandey, *J. Phys. Chem. C* **111**, 2906 (2007).
 [18] M. H. Evans, J. D. Joannopoulos and S. T. Pantelides, *Phys. Rev. B* **72**, 045434 (2005).
 [19] J. Kunstmann, and A. Quandt, *Phys. Rev. B* **74**, 035413 (2006).
 [20] I. Cabria, M. J. Lopez, and J. A. Alonso, *Nanotechnology* **17**, 778 (2006).
 [21] N. G. Szwacki, A. Sadrzadeh, and B. I. Yakobson, *Phys. Rev. Lett.* **98**, 166804 (2007).
 [22] P. Hohenberg, and W. Kohn, *Phys. Rev.* **136**, B864 (1964).
 [23] W. Kohn, and L. J. Sham, *Phys. Rev.* **140**, A1133 (1965).
 [24] M. C. Payne, M. P. Teter, D. C. Allen, T. A. Arias, and J. D. Joannopoulos, *Rev. Mod. Phys.* **64**, 1045 (1992).
 [25] PARAllel Total Energy Code (PARATEC) is a plane-wave pseudopotential program for parallel computations. <http://www.nersc.gov/projects/paratec/>
 [26] J. P. Perdew and A. Zunger, *Phys. Rev. B* **23**, 5048 (1981).
 [27] J. P. Perdew, *et al.*, *Phys. Rev. B* **46**, 6671 (1992).
 [28] P. J. Durrant and B. Durrant, *Introduction to Advanced Inorganic Chemistry*, pp. 118-121 (Wiley & Sons, New York, 1962).